Low-Temperature Optical Spectroscopy of Native and Azide-Reacted Bovine Cu,Zn Superoxide Dismutase. A Structural Dynamics Study†

Antonio Cupane,‡ Maurizio Leone,‡ Valeria Militello,‡ M. Elena Stroppolo,§ Fabio Polticelli,§,∥ and Alessandro Desideri*,§,⊥

Institute of Physics and INFM, University of Palermo, 90123-Palermo, Italy, Department of Biology, University of Rome "Tor Vergata", 00133 Rome, Italy, Radiobiology Unit, Medical Research Council, Chilton, Didcot, Oxon, OX11 0RD, UK, and Department of Organic and Biological Chemistry, University of Messina, 98166 Messina, Italy

Received May 12, 1994; Revised Manuscript Received September 27, 1994⊗

ABSTRACT: The optical absorption spectra of native and N_3^--reacted Cu,Zn superoxide dismutase (SOD) has been studied in the temperature range 300-10 K. The broad d−d bands observed in the room temperature spectrum, centered at 14 700 cm^{-1} (native enzyme) and at 15 550 cm^{-1} (N_3^--reacted enzyme), are clearly split at low temperature into two bands each, centered at 12 835 and 14 844 cm^{-1} and at 14 418 and 16 300 cm^{-1}, respectively. The thermal behavior of the 23 720 cm^{-1} band present in the spectrum of the native enzyme indicates that this band belongs to the His61→Cu(II) ligand to metal charge transfer transition. Analysis of the zeroth, first, and second moments of the various bands as a function of temperature allowed us to obtain useful information on the stereodynamic properties of the metal site in SOD. In particular for the native protein, it was possible to infer a variation in the metal ligand relative position that occurs as the temperature is lowered and that likely involves all of the ligands except His61. On the other hand, the site is stabilized upon N_3^- binding, and in this case a variation in the metal ligand position is observed only at the level of the bound anion. The possible relation of these properties to the catalytic mechanism of the enzyme is discussed.

Copper,zinc superoxide dismutases (Cu,Zn SODs)[1] are ubiquitous metalloproteins that catalyze the dismutation of superoxide (O_2^-) into oxygen and hydrogen peroxide (Bannister et al., 1987) by alternate reduction and oxidation of a Cu^{2+} ion, constituting the active redox center. The rate-limiting step of this reaction is the diffusion of superoxide toward the active site, modulated by the distribution of the protein-generated electric field, which has been found to be a conserved feature for all of the Cu,Zn SODs investigated (Desideri et al., 1992). This reaction constitutes a front-line defense against the cytotoxicity arising from biological oxygen activation (Bannister et al., 1987).

The three-dimensional structure of the Cu,Zn enzyme has been described by crystallographic analysis of five different species, namely, ox (Tainer et al., 1982), spinach (Kitagawa et al., 1991), yeast (Dijnovic et al., 1992a), human (Parge et al., 1992), and *Xenopus laevis* (Dijnovic et al., 1993). The metal cluster forming the enzyme active site is constituted by a copper atom and a zinc atom coupled together by a bridging imidazolate side chain (His61), which occupies a solvent-exposed loop of the rigid β-barrel structure of each identical subunit of the native dimeric enzyme. The Zn^{2+} ion is coordinated by two more histidyl and one aspartyl residue (His69, His78, Asp81), while the catalytically active Cu^{2+} ion is coordinated by three additional histidyl residues (His44, His46, His118) as well as by one water molecule (Tainer et al., 1982), which is in fast exchange with the bulk water (Gaber et al., 1972).

The interaction of SOD with anions has been widely studied because singly charged anions competitively inhibit the enzymatic activity, likely mimicking the enzyme−substrate interaction (Rigo et al., 1977; Sette et al., 1992). The structure of the azide-reacted bovine enzyme has been solved recently, showing that the anion binds directly to the copper atom, displaces the copper-bound water molecule, and gives rise to a square pyramidal configuration around the copper in which the apical ligand occupies an elongated position (Djinovic et al., 1994). However, in spite of the fact that proteins currently are thought to be fluctuating objects (Frauenfelder et al., 1991), and that the relevance of protein dynamics to a deeper understanding of their functional behavior is widely recognized, no data have been available up to now that can shed light on the dynamic properties of the metal active site, either in the native or in the anion-bound state.

Useful information on the structural and dynamic properties of the active site of metalloproteins may be obtained from an analysis of the trends of the electronic absorption spectra of the metal as a function of the temperature (Cordone et al., 1986; Cupane et al., 1988). In fact, the optical absorption bands of a chromophore embedded in a matrix, such as a metal bound to a protein, undergo peak frequency shift, line width narrowing, and gain or loss of integrated intensity as the temperature is lowered; these changes arise from the interaction of the optical electrons with the motions of the nearby nuclei, and therefore they contain information

† This work was supported by the EC program "Human Capital and Mobility". General indirect support from CRRNSM (Comitato Regionale Ricerche Nucleari e Struttura della Materia) to A.C., M.L., and V.M. is also gratefully acknowledged.

‡ University of Palermo.
§ University of Rome.
∥ Medical Research Council.
⊥ University of Messina.

⊗ Abstract published in *Advance ACS Abstracts,* November 1, 1994.

[1] Abbreviations: SOD, superoxide dismutase; Mops, morpholinopropanesulfonic acid; RR, resonance Raman; LMCT, ligand to metal charge transfer.

0006-2960/94/0433-15103$04.50/0

on the dynamic properties of the complex. The temperature dependence of the integrated intensity (zeroth moment), center frequency (first moment), and line width spread (second moment) of the optical absorption bands, therefore, gives information on the stereodynamic properties of the protein in the proximity of the active site.

The experimental approach outlined here, aimed at obtaining information on the dynamic properties of proteins, is of low resolution as compared to, for example, resonance Raman spectroscopy. It should be pointed out, however, that optical spectroscopy is also effective in probing absorption bands, characterized by a low extinction coefficient, that can barely be studied by resonance Raman spectroscopy. This is particularly important in the case of Cu,Zn SOD, since different bands, arising from charge transfer or d−d transitions, probe different dynamic features of the active site. Moreover, the optical spectroscopy approach enables one to obtain averaged information on the "bath" of low-frequency modes ($\nu < 200$ cm^{-1}), for which resonance Raman spectroscopy is not very sensitive. On the other hand, EPR spectroscopy may be used to probe, at a single temperature, the heterogeneity around the metal ion arising from the presence of an ensemble of protein molecules in different conformational states (Aqualino et al., 1991; Bizzarri et al., 1993), but this technique gives average information on the site and does not allow one to infer stereodynamic properties concerning specific copper ligands.

In this work, the optical absorption spectrum of native and N_3^--reacted Cu,Zn SOD has been investigated as function of temperature. In the low-temperature spectrum, the d−d transition, which is a single unresolved broad band at room temperature, is clearly split into two bands. Assignments of such bands have been carried out by taking into consideration the EPR properties and the known geometrical environment provided by the copper ligands in the native and the anion-bound protein. Moreover, analysis of the temperature dependence of the two spectra allowed us to note different dynamic properties of the active site in the native and inhibited states, which may likely be correlated with the catalytic mechanism of the enzyme.

MATERIALS AND METHODS

Bovine superoxide dismutase was purified from bovine erythrocytes as previously described (McCord & Fridovich, 1969). Samples for spectrophotometric measurements contained 3×10^{-4} M Cu,Zn SOD in 5 mM Tris−Mops buffer (pH 8) and 66% (w/w) glycerol−water. The N_3^--reacted derivative was prepared by adding NaN_3 directly to the cuvette to a final concentration of 0.3 M. To measure the charge transfer band at 26 000 cm^{-1}, the sample was diluted approximately 3-fold with the buffer solution containing 66% glycerol in water.

The experimental setup and methods for optical measurements in the temperature range 300-10 K have been described previously (Cordone et al., 1986). Spectra were recorded with a Varian 2300 spectrophotometer interfaced to an IBM PC; spectral data acquisition was performed at 1 nm steps, and the bandwidth was less than 1 nm in the whole spectral range explored. At each temperature, the absorption spectra of the cuvette plus buffer plus solvent, recorded in separate experiments, were subtracted from sample spectra.

Deconvolution of the spectra in Gaussian components was performed according to

$$A(\nu) = \sum_{k=1}^{N} I_k \exp[-(\nu - \nu_{0k})^2/2\sigma_k^2]$$

where $A(\nu)$ is the absorbance at frequency ν, I_k, ν_{0k}, and σ_k are the amplitude, peak position, and half-width of the kth component, respectively, and N is the number of components. A comment concerning the use of Gaussian bands to describe optical transitions seems to be in order here. It can be shown (Di Pace et al., 1992) that the absorption band profile is described by a sum of Voigtians (a Voigtian is the convolution of a Lorentzian with a Gaussian), whereby the Lorentzian half-width Γ takes into account the homogeneous broadening due to the nonradiative population decay of the excited electronic state, and the Gaussian line width σ takes into account both the coupling with low-frequency vibrational modes and the presence of inhomogeneous broadening. In the present case, the Gaussian term dominates the spectral shape, even at 10 K. In fact, σ values are never smaller than 700 cm^{-1} (Table 1), as compared to typical Γ values on the order of 250 cm^{-1} (Di Pace et al., 1992), so that $\Gamma < \sigma$ at all temperatures and the bands may be described as sums of Gaussians.

An HP-1000 computer was used, and the mean square deviation (χ^2) was minimized using a nonlinear least-squares algorithm (Marquardt, 1963). Errors on fitted parameters were calculated by inversion of the curvature matrix, within the approximation of parabolic χ^2 surface around the minimum; they correspond to 67% confidence limits. Within the so-called narrow band approximation (Dexter, 1958), the zeroth (M_0), first (M_1), and second (M_2) moments of a band are defined as

$$M_0 = \int_{-\infty}^{\infty} A(\nu)\, d\nu$$

$$M_1 = M_0^{-1} \int_{-\infty}^{\infty} \nu A(\nu)\, d\nu$$

$$M_2 = M_0^{-1} \int_{-\infty}^{\infty} \nu^2 A(\nu)\, d\nu - M_1^2$$

In the present case of Gaussian bands, the integrated intensity is given by $M_{0k} = [(2\pi)^{1/2} I_k \sigma_k]$, the center frequency is given by $M_{1k} = \nu_{0k}$, and the line width spread is given by $M_{2k} = \sigma_k^2$.

RESULTS AND DISCUSSION

Native Enzyme. Figure 1 (upper panel) shows the optical absorption spectra of Cu,Zn SOD from 10 000 to 30 000 cm^{-1} at 10 and 300 K. In the low-temperature spectrum, the large band centered at 14 700 cm^{-1} at room temperature clearly is split into two bands (I and II) centered at 12 835 and 14 844 cm^{-1}, respectively; moreover, an intense band, labeled IV in the spectrum, is observed at 23 720 cm^{-1}. Deconvolution of the experimental spectrum into Gaussian components (Figure 1, lower panel) indicates that a third band (band III) at 19 500 cm^{-1} must be introduced in order to obtain a good fit. A previous CD study (Pantoliano et al., 1982) had already suggested the presence of a band around 19 000 cm^{-1} and the splitting into two components, at 16 400 and 13 000 cm^{-1}, of the broad band centered at 14 700 cm^{-1}. The peak frequencies of the two bands resolved by CD spectroscopy are not exactly the same as those identified in our electronic spectrum (Figure 1 and

Table 1: Peak Position (ν_0) and Gaussian Width (σ) at $T = 10$ and 300 K for the Single Spectral Components of Native and N_3^-–SOD

		ν_0 (cm^{-1})		σ (cm^{-1})	
derivative	band	$T = 10$ K	$T = 300$ K	$T = 10$ K	$T = 300$ K
native SOD	I	12835 ± 10	12575 ± 30	741 ± 8	1271 ± 20
native SOD	II	14844 ± 15	15160 ± 60	1647 ± 10	1950 ± 30
native SOD	III	19500[a]	19500[a]	1600[a]	1600[a]
native SOD	IV	23720 ± 15	22719 ± 30	1850[a]	1850[a]
N_3^-–SOD	I	14405 ± 10	14531 ± 20	825 ± 7	1285 ± 10
N_3^-–SOD	II	16300 ± 10	16643 ± 30	1761 ± 10	2336 ± 15
N_3^-–SOD	0	12050[a]	12050[a]	729 ± 15	939 ± 15
N_3^-–SOD	LMCT	27171 ± 20	26709 ± 20	1805 ± 18	2078 ± 25

[a] Errors are not given since these parameters have been held constant in the fitting procedure.

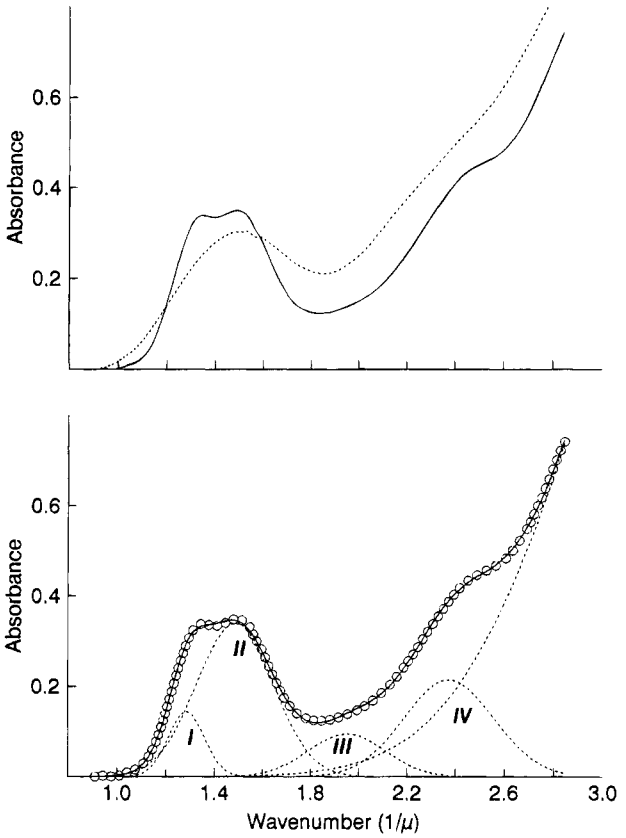

FIGURE 1: Upper panel: Optical absorption spectra of native SOD at 300 K (broken line) and at 10 K (continuous line). Lower panel: Deconvolution of the 10 K spectrum in terms of Gaussian components. Circles represent the experimental points and broken lines the Gaussian components; the overall synthesized profile is represented by continuous lines. For the sake of clarity, not all of the experimental points have been reported.

Table 1), and this may be attributed to the lower resolution of the previous experiment. As far as the exact location of the maximum of band III is concerned, it must be noted that an equally good fit of the experimental spectrum reported in Figure 1 is obtained by shifting this band from 19 000 to 19 700 cm^{-1}, so that the peak frequency of band III is subject to large uncertainty. The presence of band III is, however, unambiguous since it is always needed to have a good fit of the electronic spectrum at each temperature investigated; moreover, its existence has already been inferred by CD spectroscopy (Pantoliano et al., 1982), and it is in agreement with the rhombic EPR spectrum of the copper native site (Rotilio et al., 1972) due to a ligand field that displays considerable deviation from tetragonal symmetry, as has been evidenced by the crystallographic structure determination (Tainer, 1982; Djinovic et al., 1992).

The temperature dependence of M_0, M_1, and M_2 on bands I, II, and IV is reported in Figure 2. An analysis of the temperature dependence of band III has not been attempted since its maximum has been kept constant for all fits performed at each temperature. The integrated intensities (M_0) of bands I and II are constant over the temperature range investigated, confirming their assignment to mainly d–d transitions. In fact, temperature-induced intensity variations are expected to occur only for ligand metal charge transfer transitions, largely due to alteration of the metal ligand relative positions, which may cause a different overlap between the orbitals involved in the transition (Cordone et al., 1986; Cupane et al., 1988). This is actually the case for band IV, whose integrated intensity increases by up to 50% upon going from room temperature to 10 K (Figure 2a). This behavior classifies band IV as a charge transfer band, in agreement with previous results from a CD study (Pantoliano et al., 1982).

The M_1 and M_2 temperature dependencies have been analyzed within the harmonic Franck–Condon approximation by making use of the following expressions (Markham, 1959; Baldini et al., 1965):

$$M_1 = D + F \coth(h\langle\nu\rangle/2kT) \quad (1)$$

$$M_2 = A \coth(h\langle\nu\rangle/2kT) + \sigma_{in}^2 \quad (2)$$

where $\langle\nu\rangle$ is the mean effective frequency of the nuclear motions coupled to the electronic transition, and D, F, and A are parameters linked to the Franck–Condon linear and quadratic coupling constants; moreover, the term σ_{in}^2 in eq 2 takes into account temperature independent contributions to the bandwidth arising from conformational heterogeneity. It should be noted that eqs 1 and 2 are based on the so-called Einstein model: in order to minimize the number of adjustable parameters, this model treats the large number of low-frequency modes coupled to the electronic transition as N_1 degenerate modes of frequency $\langle\nu\rangle$ (bath of low-frequency modes); in this way, the average properties of the bath can be obtained. The M_2 temperature dependence of bands I and II is fully harmonic and may well be fit by eq 2 in the entire temperature range (Figure 2c). Large amplitude anharmonic contributions to nuclear motions have been observed for both liganded and unliganded ferrous heme proteins (Di Pace et al., 1992; Cupane et al., 1993), while completely harmonic M_2 thermal behavior has also been reported in the case of the blue copper proteins azurin and stellacyanin (Cupane et al., 1990). It is tempting to suggest that the β-barrel structure, present in both the blue copper proteins and the Cu,Zn SOD, which confers high stability to these proteins, may be responsible for the harmonic M_2 behavior.

The temperature dependence of M_1 of bands I and II follows eq 1 just up to 170 K, where a marked deviation from the regular trend occurs for both bands, although to different extents (Figure 2b). This result indicates that a structural rearrangement of the metal site, due to a protein conformational change, is occurring at this temperature. However, because of the proximity of the deviation temperature to the glassing temperature of the glycerol–water

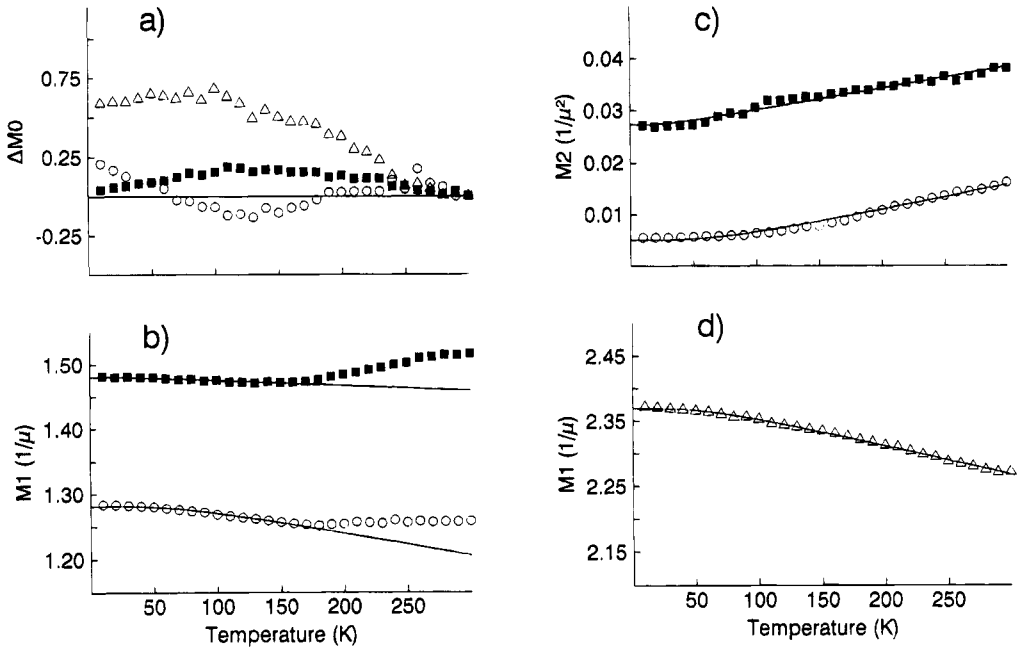

FIGURE 2: (a) Fractional variation in M_0 as a function of temperature for bands I, II, and IV of native SOD. ΔM_0 is defined as $\Delta M_0(T) = [M_0(T) - M_0(300\ K)]/M_0(300\ K)$. (b and c) M_1 and M_2 of bands I and II as a function of temperature. (d) M_1 of band IV as a function of temperature. ○, band I; ■, band II; △, band IV.

Table 2: Electron Vibrations Mean Effective Coupling Parameters of Native and N_3^-−SOD

derivative	band	$\langle\nu\rangle$ (cm^{-1})	A ($cm^{-2} \times 10^{-4}$)	σ_{in} (cm^{-1})	F (cm^{-1})	D (cm^{-1})
native SOD	I Cu d−d	140 ± 20	50 ± 10		−360 ± 10	11475 ± 8
native SOD	II Cu d−d	50 ± 8	17 ± 5	1600 ± 100	−33 ± 3	12182 ± 3
native SOD	IV, LMCT Im−Cu	120 ± 10			−390 ± 10	15518 ± 3
N_3^-−SOD	I $d_{x^2-y^2}-d_{xy}$	90 ± 15	29 ± 3	645 ± 20	33 ± 2	11989 ± 5
N_3^-−SOD	II $d_{x^2-x^2}-d_{xz},d_{yz}$	225 ± 20	260 ± 10	765 ± 60	345 ± 10	12628 ± 5
N_3^-−SOD	LMCT N_3^-−Cu	165 ± 15	60 ± 10	1800 ± 100	−324 ± 5	16522 ± 5

mixture (180 K; Ansari et al., 1987; Cordone et al., 1988), it cannot be excluded that the protein conformational rearrangement is partly coupled to the transition of the physical state of the solvent matrix. Analogous deviations present in the trend of M_1, but not in that of M_2, have already been reported for the visible bands of azurin (Cupane et al., 1990) and liganded ferrous myoglobin (Cordone et al., 1988), and they have been attributed to a conformational rearrangement of the protein that alters the electric field felt by the electron that undergoes the electronic transition, without substantially altering either the frequency of nuclear motions or their coupling constants with the electronic transition. The values of the relevant parameters obtained from the fittings are reported in Table 2 and indicate that the mean frequency of the nuclear motions coupled with band II are softer than those coupled with band I, although both are characterized by relatively low frequency. No resonance Raman (RR) work is available in the literature in order to verify the presence of such low-frequency modes; however, RR study on the blue copper proteins (Woodruff et al., 1984) or on a Cu,Zn SOD mutant in which a histidine has been replaced by a cysteine residue (Han et al., 1993) indicated the presence of several peaks ranging from 140 to 400 cm^{-1}. The low-frequency bands were attributed to ligand−Cu deformations, and the optical bands likely are coupled with these modes. It is also interesting to note that the σ_{in} values reported in Table 2 are different from zero, suggesting the existence of microheterogeneity (i.e., several different conformations) as it was also observed in azurin and stellacyanin (Cupane et al., 1990; Ehrenstein & Nienhaus, 1992).

For band IV, the M_1 thermal behavior is substantially harmonic since it may well be fit by eq 1 in the entire temperature range (Figure 2d). The M_2 trend has not been analyzed since for this band, M_2 has been kept constant in the spectral deconvolutions at all temperatures; in fact, if this constraint is not imposed, very small variations are observed without significant improvement in the overall fit.

The different thermal behavior of M_1 relative to band IV with respect to that relative to bands I and II needs to be discussed. In fact, it is clear from the deviation of M_1 of bands I and II that at about 170 K a deformation is occurring at the level of the protein metal site; however, M_1 of band IV does not feel such a rearrangement. In our opinion, this is possible only if band IV arises from a ligand to metal charge transfer (LMCT) transition in which the imidazole of His61, which bridges the copper and zinc atoms, is involved. In this case, in fact, the deformation felt by the copper site may not include His61, which is rigidly anchored

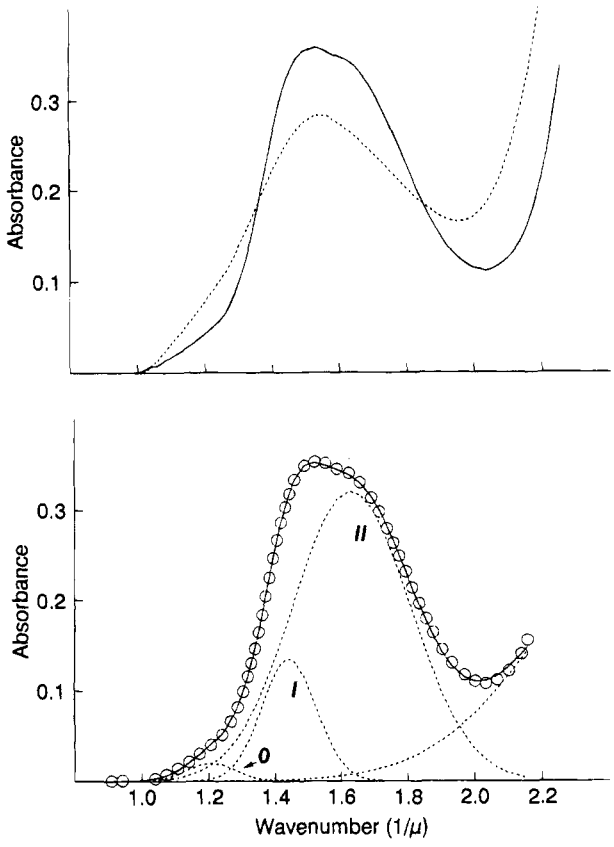

FIGURE 3: Upper panel: Optical absorption spectra of N_3^--reacted SOD at 300 K (broken line) and at 10 K (continuous line). Lower panel: Deconvolution of the 10 K spectrum into Gaussian components. Symbols and conditions as for Figure 1.

to the deeply buried zinc atom. The 23 720 cm^{-1} band must then belong to a LMCT transition involving the imidazolate group of His61, as already suggested by a CD study (Pantoliano et al., 1982), on the basis of similarities with the spectra of model compounds.

N_3^--Reacted Enzyme. The electronic spectrum of the azide derivative of Cu,Zn SOD has been investigated in two different sets of experiments, with samples having different concentrations because of the high extinction coefficient of the Cu−N_3^- charge transfer band at about 26 700 cm^{-1} (Morpurgo et al., 1973). Figure 3 (upper panel) shows the optical absorption spectrum of an N_3^--bound SOD derivative from 10 000 to 22 000 cm^{-1} at 10 and 300 K. Lowering the temperature produces a splitting of the broad band at 15 000 cm^{-1}; this splitting, although it is not so pronounced as the one observed in the native enzyme, enables us to solve two bands centered at 14 418 and 16 300 cm^{-1}, respectively (Figure 3 and Table 1). A previous room-temperature CD study indicated the presence of two bands: the first in line with our result at 14 300 cm^{-1} and the second at 18 500 cm^{-1} (Bertini et al., 1985). Upon an increase in the temperature, a shift toward higher energy is actually observed for band II (16 643 cm^{-1} at 300 K), but we can confidently exclude the presence of such a band at 18 000 cm^{-1}. The recently solved X-ray structure of the N_3−SOD derivative has shown that the copper is coordinated into a square pyramidal symmetry, with an elongation of the endogenous apical ligand (Djinovic et al., 1994). In agreement, the EPR spectrum has an axial shape (Rotilio et al., 1972) and the two electronic bands may be attributed to the $d_{x^2-y^2} \rightarrow d_{xy}$ and $d_{x^2-y^2} \rightarrow d_{xz},d_{yz}$ transitions. The best fit of the 10 K spectrum, shown in the lower panel

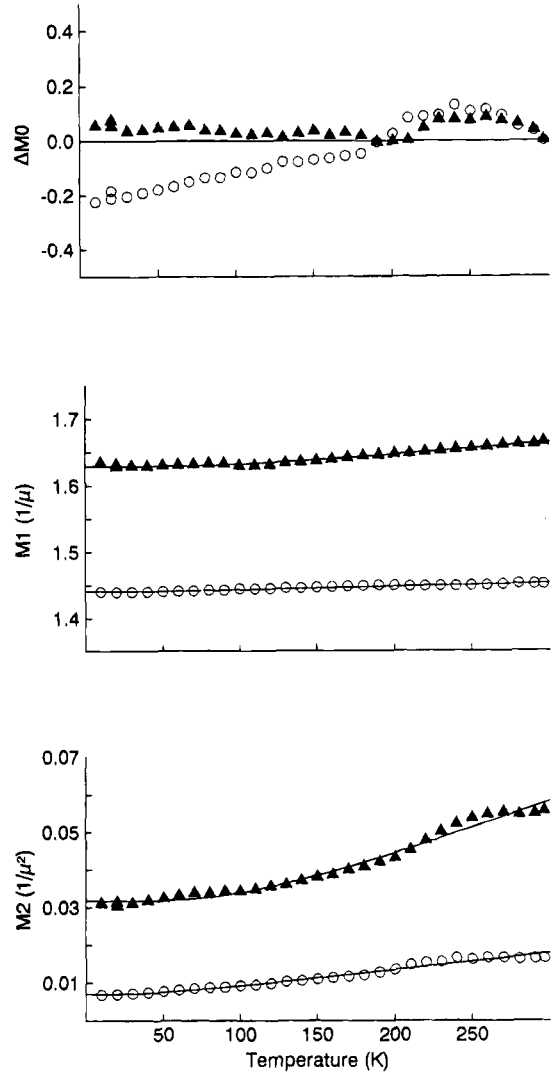

FIGURE 4: ΔM_0 (top panel), M_1 (central panel), and M_2 (bottom panel) of bands I and II of SOD−N_3^- as a function of temperature. ○, band I; ▲, band II.

of Figure 3, indicates the presence of a new band at 12 050 cm^{-1} characterized by a very low extinction coefficient. This band (labeled 0 in the figure) may be assigned as a $d_{x^2-y^2} \rightarrow d_{z^2}$ transition since such a low-energy band has been observed in square pyramidal and octahedral model compounds having elongated apical ligands (Hataway & Billing, 1970).

The temperature dependencies of M_0, M_1, and M_2 of bands I and II (Figure 4) display different behavior with respect to that observed in the native enzyme. In fact, the integrated intensities are practically constant over the entire temperature range investigated, and the M_1 and M_2 trend is harmonic and may well be fit by eqs 1 and 2. It is interesting to note that the M_1 deviations at about 170 K, observed in the native enzyme (Figure 2), are completely absent from the anion-bound derivative (Figure 4), suggesting that binding of the exogenous inhibitor increases the overall stability of the metal site. Azide is actually known to bind to the active site by replacing the metal-bound water molecule (Rigo et al., 1977), which is in fast exchange with the bulk water (Fee & Gaber, 1972; Terenzi et al., 1974), and by forming a weak hydrogen bond with the guanidinium group of the nearby Arg141 (Djinovic et al., 1994). The screening of the active site from the bulk water and the formation of an ion pair may contribute to stabilize the catalytic copper site. Values of

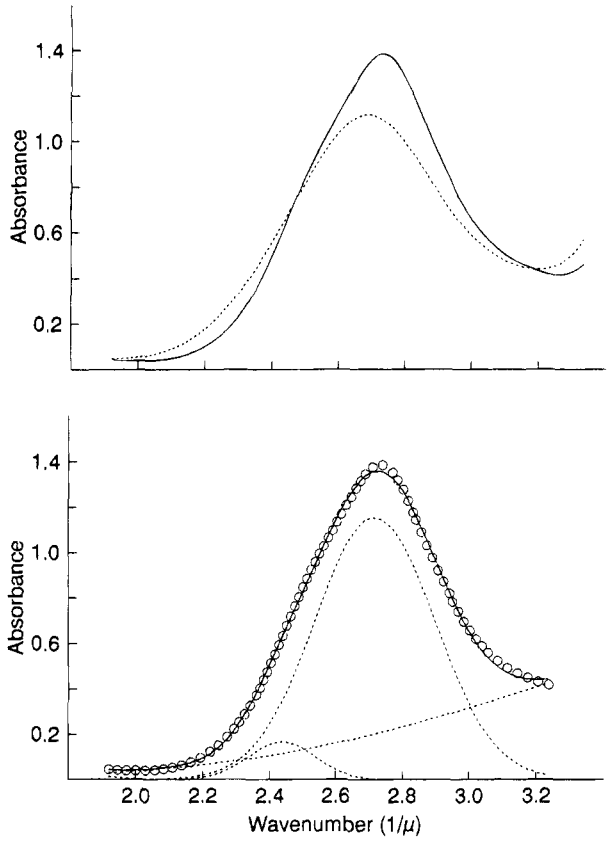

FIGURE 5: Upper panel: Optical absorption spectra of N_3^--reacted SOD in the charge transfer region at 300 K (broken line) and at 10 K (continuous line). Lower panel: Deconvolution of the 10 K spectrum into Gaussian components. Symbols and conditions as for Figure 1.

the relevant parameters obtained from the fits are reported in Table 2 and indicate that bands I and II are coupled with metal−ligand deformation modes whose mean effective frequencies are about 90 and 200 cm^{-1}, respectively, again in the range of characteristic modes of metal−ligand deformation (Woodruff et al., 1984).

Figure 5 (upper panel) shows the spectrum of N_3^--reacted SOD in the frequency range 20 000−32 000 cm^{-1} at 10 and 300 K; the deconvolution of the 10 K spectrum in terms of Gaussian components is shown in the lower panel of Figure 5. The intense peak at ≈26 700 cm^{-1} in the room-temperature spectrum and attributed to a Cu→N_3^- charge transfer transition (Morpurgo et al., 1973) clearly shows a composite structure in the 10 K spectrum. In fact, it also contains a band at ≈24 000 cm^{-1}, which, in analogy with the native derivative, can be attributed to a LMCT transition involving the imidazole of His61. Due to the presence of the nearby very intense Cu−N_3^- charge transfer band, the ≈24 000 cm^{-1} band is never resolved in the spectrum. For this reason, we did not attempt to analyze the temperature dependence of the two bands separately; on the contrary, we studied the thermal behavior of a superposition of the two Gaussians shown in Figure 5. The behavior of this sum is expected to reflect that of the Cu−N_3^-, charge transfer transition, in view of its much larger intensity. The M_0, M_1, and M_2 temperature dependencies are shown in Figure 6. The integrated intensity is pretty constant from 10 up to around 170 K, when it starts to decrease sharply, reaching 25% of the original value at 10 K; at the same temperature, M_1 shows a clear deviation from eq 1 while M_2 remains

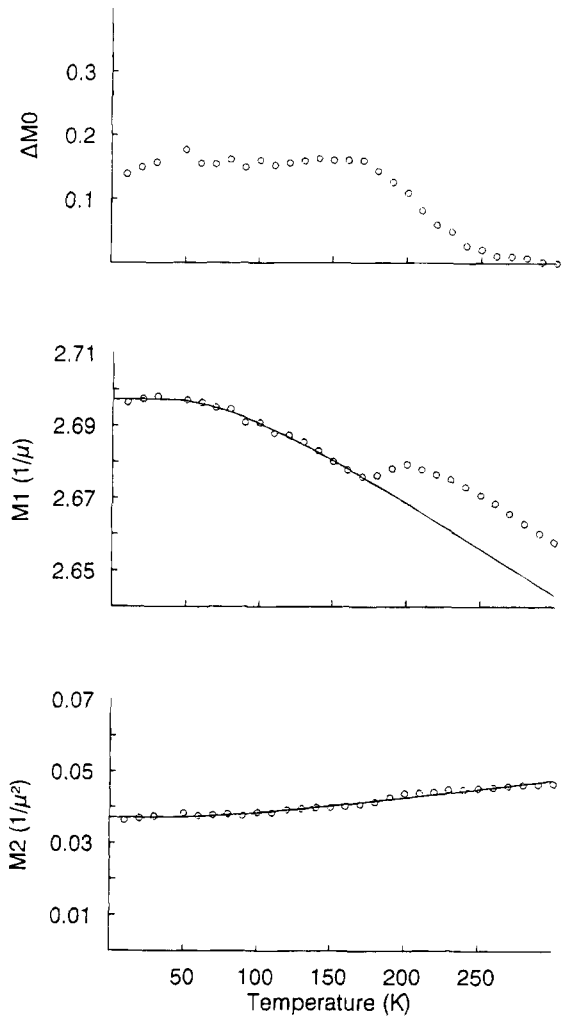

FIGURE 6: ΔM_0 (top panel), M_1 (central panel), and M_2 (bottom panel) of the charge transfer band of SOD−N_3^- as a function of temperature. Moments reported here refer to the single band arising from the sum of the two Gaussian components shown in Figure 5.

harmonic over the entire temperature range (Figure 6). This behavior may again be rationalized by a conformational readjustment of the protein that starts at about 170 K; however, because of the harmonic behavior of M_1 and M_2 relative to bands I and II, the rearrangement must involve only the exogenous anion. This interpretation would explain both the difference observed at the level of the integrated intensity, due to a different metal−ligand orbital overlap, and the deviation of M_1 for the LMCT band.

CONCLUSIONS

Measurement of the 10 K spectra of native and N_3^--bound SOD derivatives enabled us to solve the bands, of which the spectrum is composed. In particular, in the N_3^--bound derivative it has been demonstrated for the first time that the broad band centered at about 15 000 cm^{-1} in the room-temperature spectrum is actually composed of two components centered at 14 405 and 16 300 cm^{-1}. A splitting of the broad band at 14 700 cm^{-1} has also been detected for the native enzyme, and although already hypothesized by a CD study (Pantoliano et al., 1982), the peak frequencies of the two components have been more clearly defined in this work. Moreover, in the native spectrum, the assignment of the 24 000 cm^{-1} band to the His61 Im→Cu(II) LMCT transition has been confirmed.

The thermal behavior of the bands has indicated that a structural rearrangement at the level of the metal site is occurring in both the native and anion-bound enzymes at about 170 K. However, while in the native enzyme such rearrangement involves all of the copper ligands except His61, in the azide-bound derivative it involves just the copper-bound anion. Such different dynamic properties may have functional relevance, since azide is a competitive inhibitor of Cu,Zn superoxide dismutase (Rigo et al., 1977), and the characterization of its way of binding to the copper may help in elucidating the substrate−enzyme interaction. The active site appears to be more mobile in the native enzyme, ready to undergo structural deformation in order to better accommodate the external inhibitor or substrate. Once the substrate is bound, the copper is tightly fixed by the internal ligands in order to perform the electron transfer reaction and only the external molecule (substrate or inhibitor) may modulate its position, in line with the fact that once the redox reaction has occurred the substrate must be released from the metal site.

ACKNOWLEDGMENT

We are indebted to Profs. Giuseppe Rotilio and Lorenzo Cordone for useful discussions and to Mr. G. Lapis for technical help.

REFERENCES

Ansari, A., Berendzen, J., Braunstein, D., Cowen, B. R., Frauenfelder, H., Hong, M. K., Iben, I. E. T., Johnson, J., Ormos, P., Sauke, T. B., Scholl, R., Shulte, A., Steinbach, P. J., Vittitow, J., & Young, R. D. (1987) *Biophys. Chem. 26*, 337−355.

Aqualino, A., Brill, A. S., Bryce, G. F., & Gerstman, B. S. (1991) *Phys. Rev. A 44*, 5257−5271.

Baldini, G., Mulazzi, E., & Terzi, N. (1965) *Phys. Rev. A 140*, 2094−2101.

Bannister, J. V., Bannister, W. H., & Rotilio, G. (1987) *CRC Biochem. 22*, 111−180.

Bertini, I., Luchinat, C., & Monnanni, R. (1985) *J. Am. Chem. Soc. 107*, 2178−2179.

Bizzarri, A. R., Bacci, M., & Cannistraro, S. (1993) *Biophys. Chem. 46*, 117−129.

Cordone, L., Cupane, A., Leone, M., & Vitrano, E. (1986) *Biophys. Chem. 24*, 259−275.

Cordone, L., Cupane, A., Leone, M., Vitrano, E., & Bulone, D. (1988) *J. Mol. Biol. 198*, 213−218.

Cupane, A., Leone, M., Vitrano, E., & Cordone, L. (1988) *Biopolymers 27*, 1977−1997.

Cupane, A., Leone, M., Vitrano, E., & Cordone, L. (1990) *Biophys. Chem. 38*, 213−224.

Cupane, A., Leone, M., & Vitrano, E. (1993) *Eur. Biophys. J. 21*, 385.

Desideri, A., Falconi, M., Polticelli, F., Bolognesi, M., Djinovic, K., & Rotilio, G. (1992) *J. Mol. Biol. 223*, 337−342.

Dexter, D. L. (1958) in *Solid State Physics* (Seitz, F., & Turnbull, D., Eds.) Academic Press, New York.

Dijnovic, K., Gatti, G., Coda, A., Antolini, L., Pelosi, G., Desideri, A., Falconi, M., Marmocchi, F., Rotilio, G., & Bolognesi, M. (1992a) *J. Mol. Biol. 225*, 791−809.

Dijnovic, K., Coda, A., Antolini, L., Pelosi, G., Desideri, A., Falconi, M., Rotilio, G., & Bolognesi, M. (1992b) *J. Mol. Biol. 226*, 227−238.

Dijnovic, K., Carugo, K., Collyer, C., Coda, A., Carri', M. T., Battistoni, A., Bottaro, G., Polticelli, F., Desideri, A., & Bolognesi, M. (1993) *Biochem. Biophys. Res. Commun. 194*, 1008−1011.

Dijnovic, K., Carugo, K., Polticelli, F., Desideri, A., Rotilio, G., Wilson, K. S., & Bolognesi, M. (1994) *J. Mol. Biol.* (in press).

Di Pace, A., Cupane, A., Leone, M., Vitrano, E., & Cordone, L. (1992) *Biophys. J. 63*, 475−484.

Ehrenstein, D., & Nienhaus, G. U. (1992) *Proc. Natl. Acad. Sci. U.S.A. 89*, 9681−9685.

Fee, J. A., & Gaber, B. P. (1972) *J. Biol. Chem. 247*, 60−65.

Frauenfelder, H., Sligar, S. G., & Wolynes, P. G. (1991) *Science 254*, 1598.

Gaber, B. P., Brown, R. D., Koening, S. H., & Fee, J. A. (1972) *Biochim. Biophys. Acta 271*, 1−5.

Han, J., Loehr, T. M., Lu, Y., Valentine, J. S., Averill, B. A., & Sanders-Loehr, J. (1993) *J. Am. Chem. Soc. 115*, 4256−4263.

Hataway, B. J., & Billing, D. E. (1970) *Coord. Chem. Rev. 5*, 143−207.

Kitagawa, Y., Tanaka, N., Hata, Y., Kusonoki, M., Lee, G., Katsube, Y., Asada, K., Aibara, S., & Morita, Y. (1991) *J. Biochem. 109*, 477−485.

Markham, J. J. (1959) *Rev. Mod. Phys. 31*, 956−989.

Marquardt, D. W. (1963) *J. Soc. Ind. Appl. Math. 11*, 431−441.

McCord, J., & Fridovich, I. (1969) *J. Biol. Chem. 244*, 6049−6055.

Morpurgo, L., Giovagnoli, C., & Rotilio, G. (1973) *Biochim. Biophys. Acta 322*, 204−210.

Pantoliano, M. W., Valentine, J. S., & Nafie, L. A. (1982) *J. Am. Chem. Soc. 104*, 6310−6317.

Parge, H. E., Hallewell, R. A., & Tainer, J. A. (1992) *Proc. Natl. Acad. Sci. U.S.A. 89*, 6109−6113.

Rigo, A., Stevanato, R., Viglino, P., & Rotilio, G. (1977) *Biochem. Biophys. Res. Commun. 79*, 776−783.

Rotilio, G., Morpurgo, L., Giovagnoli, C., Calabrese, L., & Mondovi', B. (1972) *Biochemistry 11*, 2187−2192.

Sette, M., Paci, M., Desideri, A., & Rotilio, G. (1992) *Biochemistry 31*, 12410−12415.

Tainer, J. A., Getzoff, E. D., Beem, K. M., Richardson, J. S., & Richardson, D. C. (1982) *J. Mol. Biol. 160*, 181−217.

Terenzi, M., Rigo, A., Franconi, C., Mondovi', B., Calabrese, L., & Rotilio, G. (1974) *Biochim. Biophys. Acta 351*, 230−236.

Woodruff, W. H., Norton, K. A., Swanson, B. I., & Fry, H. A. (1984) *Proc. Natl. Acad. Sci. U.S.A. 81*, 1263−1267.